A Phase Diagram for the Binary Blends of Nearly Symmetric Diblock Copolymers. 1. Parameter Space of Molecular Weight Ratio and Blend Composition†

Daisuke Yamaguchi and Takeji Hashimoto*

Department of Polymer Chemistry, Graduate School of Engineering, Kyoto University, Kyoto 606-8501, Japan

Received December 18, 2000; Revised Manuscript Received May 25, 2001

ABSTRACT: A phase diagram as a function of molecular weight ratio and blend composition was constructed for the binary blends of nearly symmetric polystyrene-*block*-polyisoprene (PS−PI) copolymers. In this study we prepared four series of binary blends, and every blend consists of a copolymer, hereafter designated as α, whose number-average molecular weight (M_n) and volume fraction of PS-block (f_{PS}) are 1.0×10^5 and 0.47, respectively. Four PS−PI copolymers (hereafter designated β), each of which is blended with α, have their M_n and f_{PS} in the range 1.2×10^4−2.1×10^4 and 0.40−0.49, respectively, and therefore the molecular weight ratio of α to β, hereafter designated as r, ranges between 4.8 and 8.3. All the blends showed partial miscibility of the constituent copolymers; that is, at a certain blend composition the macrophase separation between α and β occurred. However, the range of blend compositions where the constituent copolymers phase-separate became small as r decreased. As for the two blend series where $r = 4.8$ and 6.9, the PS cylindrical morphology was observed over wide blend compositions, although the constituent copolymers have nearly symmetric compositions and by themselves are self-assembled into lamellar morphology.

I. Introduction

An enormous number of studies have been reported on phase transitions and morphologies of self-assembled structures in block copolymers composed of two components (e.g., AB diblock, ABA triblock, $(AB)_n$ starblock) as well as blends of block copolymers with homopolymers or another block copolymers due to their considerable importance in both fundamental studies and commercial applications.[1−5] It should be also noted that the morphological studies of ternary (ABC) block copolymer systems have made remarkable progress in recent years.[1,6−12] In this study we discuss the self-assembled structures in binary mixtures of block copolymers. We consider here binary blends of (A−B) block copolymers α and β having different degrees of polymerization and/or volume fractions of A component (f_A). We designate hereafter α and β as the block copolymers having large and small molecular weights, respectively. These blends have two kinds of phase transitions: one is microphase transition inherent in block copolymers, and the other is macrophase transition inherent in mixtures, the interplay of which will create a variety of morphologies and even multilevel ordering as well for some cases.[13−15] Key physical parameters here are a competing interaction between short-range segmental interactions of A and B and long-range interactions of A and B originating from the connectivity of A and B. These short- and long-range interactions are inherent in block copolymers. On top of these competing interactions we have a competing long-range interaction between α and β block copolymers which is anticipated to give intriguing delicate effects on microdomain structures.

Table 1. Characteristics of PS−PI Diblock Copolymers

code	M_n[a,b]	M_w/M_n[a]	$M_{n,PS}-M_{n,PI}$[a,c]	f_{PS}[d]	morphology	r[e]
α	1.0×10^5	1.16	5.0×10^4−5.0×10^4	0.47	lamella	
β_1	1.21×10^4	<1.05	6.3×10^3−5.8×10^3	0.49	disorder	8.3
β_2	1.36×10^4	<1.05	7.1×10^3−6.5×10^3	0.49	lamella	7.4
β_3	1.45×10^4	<1.05	7.0×10^3−7.5×10^3	0.45	lamella	6.9
β_4	2.1×10^4	<1.05	9×10^3−1.2×10^4	0.40	lamella	4.8

[a] Measured by GPC. [b] M_n is number-average molecular weight. [c] $M_{n,k}$ is number-average molecular weight of the kth block (k = PS or PI). [d] f_{PS} is volume fraction of PS block chain and given by $f_{PS} = (w_{PS}/\rho_{PS})/((w_{PS}/\rho_{PS}) + (w_{PI}/\rho_{PI}))$ where $w_k = M_{n,k}/M_n$ (k = PS or PI), $\rho_{PS} = 1.0514$ g cm^{-3}, and $\rho_{PI} = 0.925$ g cm^{-3}. ρ_{PS} and ρ_{PI} are the densities of PS and PI block chain, respectively. [e] r is the molecular weight ratio between α and β_i.

For example, one may be able to consider the following five possible states of the mixtures of α and β: both block copolymers are in the disordered phase, forming either (i) a single phase or (ii) two phases, (iii) α and β are phase-separated with α in the ordered phase and β in the disordered phase, or both α and β are in the ordered phase, forming either (iv) two macroscpically phase-separated structure or (v) a single phase structure. It is of worthy to note that the self-assembly involving the mixtures of α and β is quite analogous to that involving the mixtures of thermotropic liquid crystal polymers having different rigidities due to molecular weight difference and/or to the composition difference in mesogenic groups.[16]

Let us consider the last case of (v) described above where α and β are mixed on the molecular level and form the single ordered phase. One of the new aspects in this case is that the system has less translational entropy in the case when β blocks are segregated with their junctions at the interface compared with the blends of A−B/A homopolymer, for example.[13,17−19] Thus, the system in this case has a greater contribution of stretching free energy. As an intriguing consequence

† Presented in part at the 47th Symposium of the Society of Polymer Science, Japan, Oct 1997. *Polym. Prepr. Jpn., Soc. Polym. Sci., Jpn.* **1997**, *46*, 2649−2650.

* To whom correspondence should be addressed.

10.1021/ma0021489 CCC: $20.00
Published on Web 07/27/2001

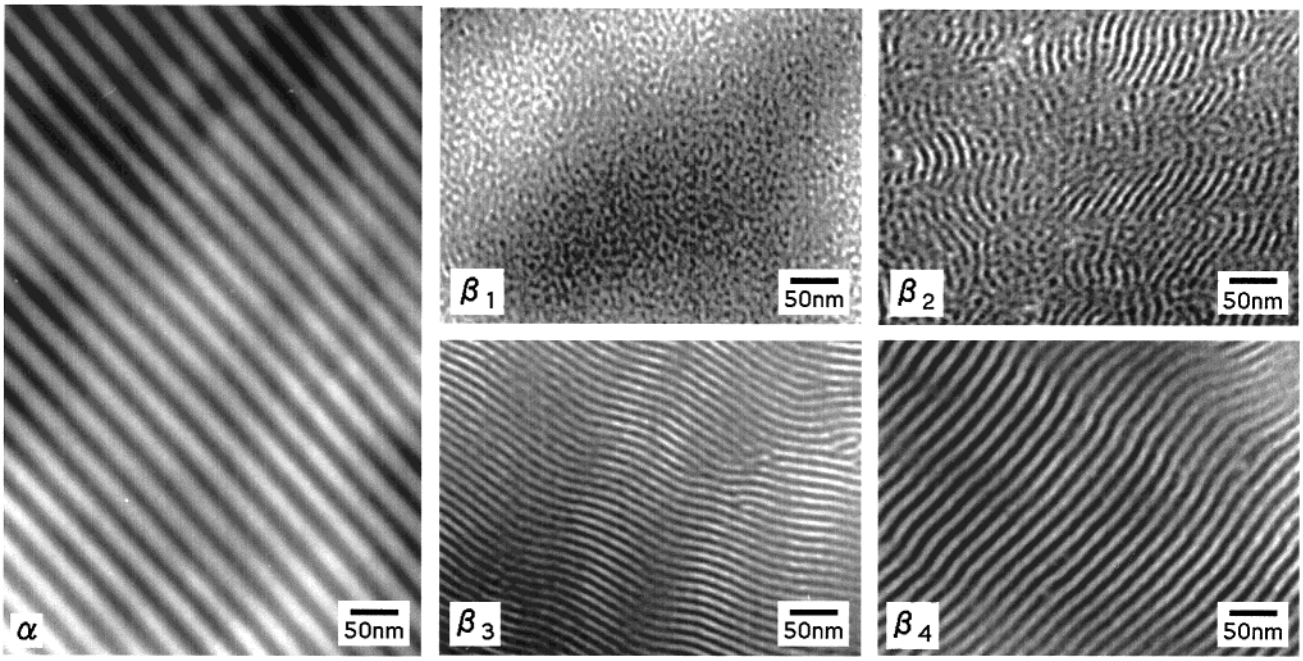

Figure 1. TEM micrographs for neat PS−PI copolymers, α and β_i ($i = 1-4$).

of this effect, we can think of a cosurfactant effect.[3, 20−24] Consider long asymmetric block copolymers α which alone form sphere or cylinders. Adding a small amount of short symmetric block copolymers, β, to the systems effectively alters interface curvatures, and hence morphology, e.g., from cylinders to lamellae, to attain uniform segmental density in space, in the case when β are molecularly mixed with α and their chemical junctions are localized at the interface of ordered microdomains.[23,24]

Thus, the problems concerning the mixtures of block copolymers are intriguing, but the systems have six independent parameters: the volume fractions of each block copolymer and their degree of polymerization as well as blend composition Φ_α and temperature T. We need a lot of works to cover systematically the whole parameter space.

Here we cite an interesting example of previous works reported on mixtures of lamella-forming polystyrene (PS)-*block*-polyisoprene (PI) (PS−PI) copolymers.[13] If a ratio r of molecular weights of α and β is smaller than 5, they show total miscibility and undergo microphase separation only forming a single lamellar phase with the lamellar spacing varying with the blend compositions. However, if $r > 10$, they undergo macrophase separation, forming coexisting grains of large lamellae L_1 and those of small lamellae L_2. We believe that the macrophase separation occurs because an equilibrium amount of β which can be solubilized in the lamellar phase of α is limited when α starts to order into lamellae (the macrophase separation induced by the microphase separation).[13] One might be skeptical at first about the reported results on macrophase separation, simply because the two block copolymers α and β have almost the same composition, and therefore the effective thermodynamic interaction parameters between them in a mixture where both α and β are in the disordered state are very small so that no macrophase separation is well expected to occur between the disordered α and β. Thus, one suspected that the macrophase separation might possibly occur due to a solvent effect in the sample preparation or some kinetic effects encountered in the

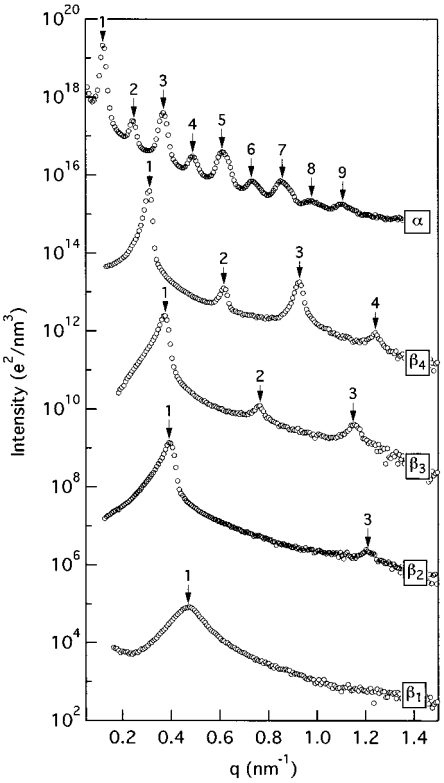

Figure 2. SAXS profiles for neat PS−PI copolymers. The intensity is shown in logarithmic scale. The profiles of α, β_4, β_3, and β_2 have been shifted vertically relative to that of β_1 by the factor of 10^{12}, 10^9, 10^6, and 10^3, respectively for clarity. The scattering peaks are marked by arrows and numbers that designate the positions relative to that of the first-order scattering peak.

solvent evaporation process. The solvent used in the above study is toluene which is well-known to be a neutral solvent for both PS and PI block chains, and hence increasing polymer concentration is equivalent to decreasing temperature for the molten mixtures of the α and β block copolymers with nearly identical glass transition temperature. Thus, the solvent effect and the

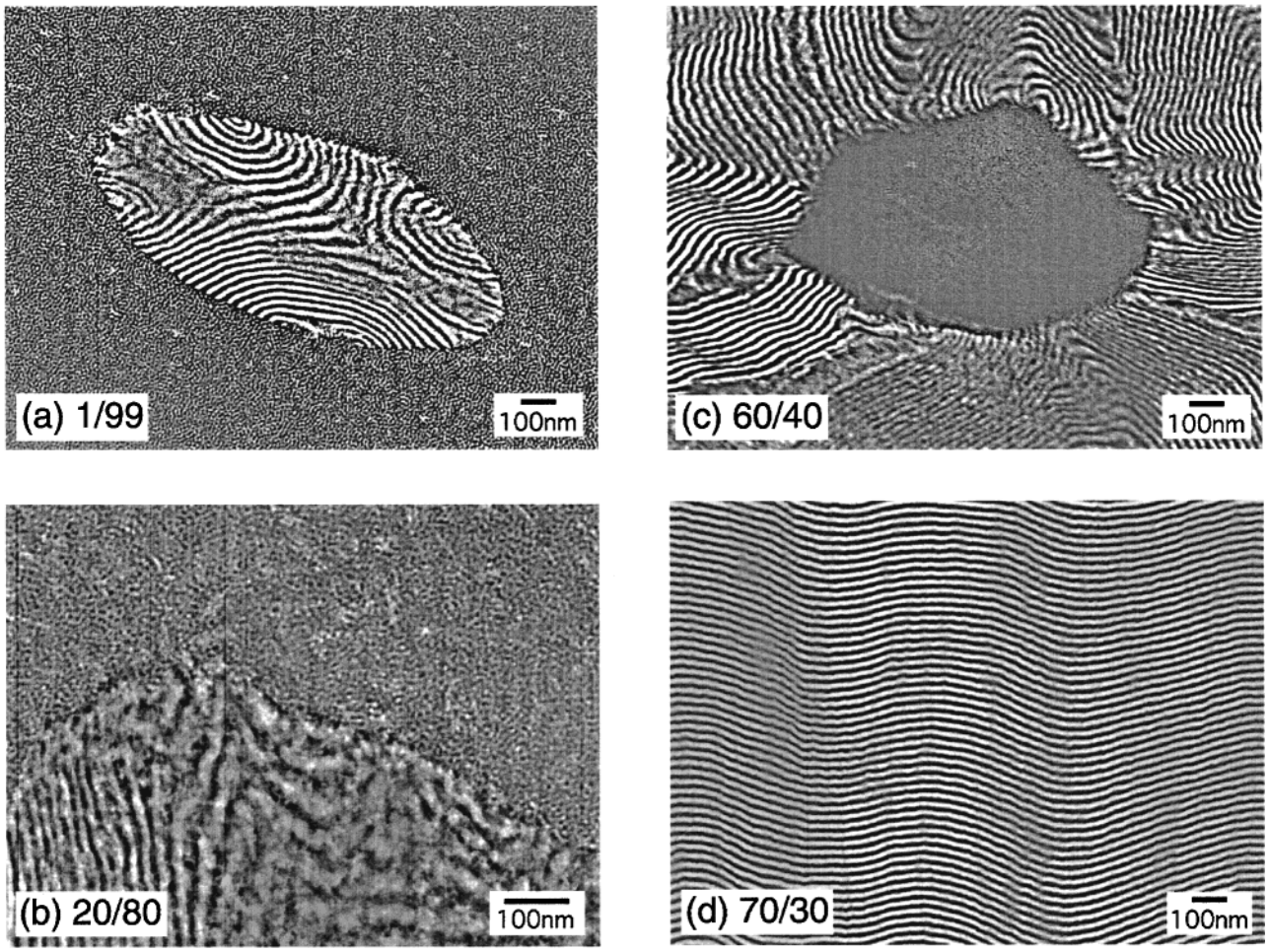

Figure 3. TEM micrographs of α/β_1 blends ($r = 8.3$). The blend compositions are designated in wt %. (a) 1/99 blend; (b) 20/80 blend; (c) 60/40 blend; (d) 70/30 blend.

kinetic effect do not seem to be a plausible scenario for the macrophase separation. Matsen theoretically confirmed later on the existence of macrophase separation at thermal equilibrium.[25] Further, the experimental studies of Lin et al.,[26] Kane et al.,[27] and Papadakis et al.[28] revealed some new aspects of binary mixtures of symmetric block copolymers with different molecular weight. However, there seems still lacking the experimental results in the intermediate range of r for the molecular weight ratio, that is, $5 < r < 10$. Therefore, in this study we investigated the region of $5 < r < 10$ on the binary mixtures of lamella-forming PS−PI copolymers and addressed the question of how the immiscible blend composition range changes with r.

II. Experimental Section

II.1. Sample Preparation. Five PS−PI's used in this study were synthesized by living anionic polymerization with *sec*-butyllithium as an initiator and cyclohexane as a solvent. The polymer molecular weight was characterized by GPC. In each synthesis a precursory PS sample was taken out before the second step polymerization of PI to determine the molecular weight of the PS block by GPC. GPC was calibrated with not only standard PS homopolymers but also PI standard homopolymers to determine correctly the molecular weight of both PI and PS block correctly. Moreover, we have a piece of evidence that the volume fraction of PS (f_{PS}) characterized by GPC during synthesis coincides with that characterized by ^{1}H NMR (for β_3 copolymer).[29] Characteristics of these copolymers are summarized in Table 1, where one long diblock copolymer, designated as α, was blended with each of the remaining short diblock copolymers, β_i ($i = 1-4$). It should be noted here that although the molecular weights of the short diblock copolymers used are ranging over a relatively narrow range (from 1.21×10^4 to 2.1×10^4), we could distinguish them correctly by the elution time of GPC. The blend specimens of α/β_i ($i = 1-4$), employed in this study, were prepared by casting from a 5 wt % polymer in toluene solution. 0.5 wt % of antioxidant (Irganox 1010, Ciba-Geigy Group) was added to the solution to prevent the thermal degradation of the specimens during the annealing of the specimens above the glass transition temperature (T_g) of PS block (∼100 °C). After the casting process, the blend specimens were annealed at 120 °C for several hours under a nitrogen atmosphere to achieve the equilibrium morphology and then gradually cooled (10 °C decrement per hour) to ambient temperature. The blend samples with different blend compositions were prepared and are designated as the weight ratio of α to β_i.

II.2. Small-Angle X-ray Scattering. For each neat diblock copolymer and blend specimen small-angle X-ray scattering (SAXS) was measured at room temperature with a SAXS apparatus described elsewhere, except for the replacement of the X-ray generator with a new one (MAC Sciences M18X HF operated at 18 kW).[30−32] SAXS profiles were corrected for air scattering, absorption, and thermal diffuse scattering.[30−32] The absolute intensity was obtained by the nickel-foil method.[33]

II.3. Transmission Electron Microscopy. Microphase- or macrophase-separated morphologies of blend specimens were observed by transmission electron microscopy (TEM). For TEM observation, the film specimens were microtomed at −100 °C, using a Reichert Ultracut E low-temperature sectioning system. The ultrathin sections were stained with the vapor of 2% OsO_4(aq) for a few hours.[34,35] Electron microscope observation was done with a Hitachi H-600S transmission

electron microscope operated at 75 kV and in the bright field mode.

III. Results

III.1. Neat Diblock Copolymers. TEM micrographs for neat diblock copolymers, α and β_i ($i = 1-4$), are shown in Figure 1. Note that in all TEM micrographs in this study PI-rich domains appear dark due to the preferential staining with OsO_4. All of the neat diblock copolymers except for β_1 show lamellar morphology, which is consistent with their nearly symmetric compositions. β_1 is in the disordered state since they have relatively low molecular weight, and the segregation power between PS and PI blocks is not sufficient to form ordered microdomains.

The morphologies of neat copolymers are further confirmed by SAXS, as shown in Figure 2. The scattering intensity are plotted in a semilogarithmic scale against the magnitude of the scattering vector, q, defined by $q \equiv (4\pi/\lambda)\sin(\theta/2)$ with λ and θ being the wavelength of the incident X-ray and the scattering angle, respectively. The agreements between SAXS and TEM results are very nice. As for the neat copolymers, α, β_2, β_3, and β_4, the higher-order scattering maxima locate at the positions of integer multiples of the position of first-order scattering maximum, q_m, indicating that copolymer chains are in the ordered state and forming alternating lamellar microdomains. Whereas in the SAXS profile of β_1, there is only one broad scattering maximum, indicating that β_1 is in the disordered state. Thus, all the neat copolymers examined here, which cover the composition range of $0.40 \le f_{PS} \le 0.49$ where f_{PS} denotes the volume fraction of PS block, are symmetric to form a lamellar morphology in their ordered sate.

III.2. Blend Specimens. *(a) α/β_1 Blend Series ($r = 8.3$).* The results of TEM and SAXS, presented in Figures 3 and 4, respectively, consistently showed that α and β_1 undergo macrophase separation into β-rich disordered phase (Dis_2) and α-rich lamellar phase (L_1) when $\Phi_\alpha \le 0.6$ while α and β_1 are totally miscible and form single ordered lamellar phase (L_1) when $\Phi_\alpha \ge 0.7$. Note that hereafter the weight fraction of α copolymer in the blend specimens is designated as Φ_α, for the sake of convenience. The miscibility criterion for α/β_1 blends fits to the results of the previous study[13] as discussed later.

The following observations in Figures 3 and 4 are worthy to note: (1) In Figure 3 even α/β_1 = 1/99 (w/w) blend clearly shows the coexistence of L_1 phase and Dis_2 phase, indicating that only very little amount of α can dissolve into short β_1 copolymer phase, and hence most of α segregate themselves into an independent phase. (2) Naturally, the volume fractions of Dis_2 and L_1 phases definitively depend on the blend composition, and quite impressively the phase inversion occurs between the 1/99 and the 60/40 blends (cf. Figure 3a,c). (3) In most case the lamellar microdomains of α-rich phase are arranged in such a way that the lamellar edges are normal to the macrointerface between the α and β_1 phases in order to minimize the free energy at the interface between the α and β_1 phases, regardless of which macrophase is a dispersed phase or a matrix phase (cf. Figure 3a,b with Figure 3c). This result is consistent with those of previous reports.[13,14] (4) In Figure 4 the first-order scattering maximum of L_1 phase in the 5/95 or 20/80 blend locates at smaller q than that of 60/40 or 70/30 blend, suggesting that the lamellar spacing of L_1 phase in 5/95 or 20/80 blend is larger than that of 60/40 or 70/30 blend. (The plots of $D = 2\pi/q_m$ as a function of Φ_α will be presented later in Figure 15.) We shall discuss this somewhat counterintuitive result later in section IV.3.

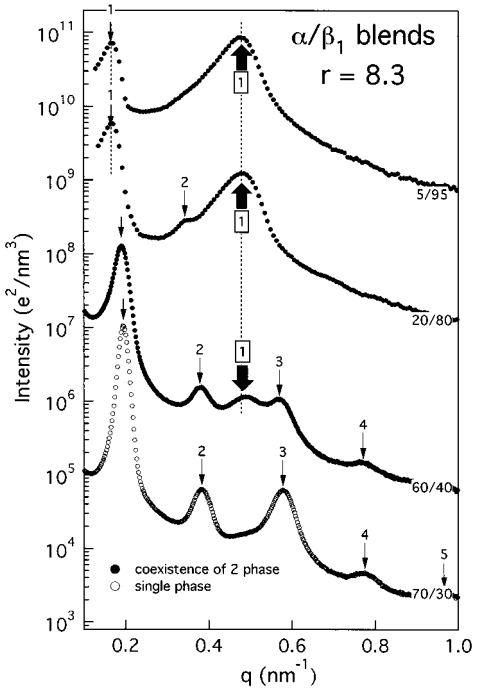

Figure 4. SAXS profiles of α/β_1 blends ($r = 8.3$). The profiles of 5/95, 20/80, and 60/40 blends have been shifted vertically relative to that of 70/30 blend by the factor of 2×10^5, 4×10^3, and 20, respectively for clarity. The profiles showing macrophase separation between α and β_1 are denoted by filled circle (●), while those showing single microphse-separated structure are denoted by open circle (○). The scattering peaks from α-rich phase are marked by thin arrows and numbers without boxes, while those from β_1-rich phase are indicated by thick arrows and numbers with boxes. The number indicates the positions relative to that of the first-order scattering peak.

(b) α/β_2 Blend Series ($r = 7.4$). As for the α/β_2 blend whose TEM and SAXS results are presented in Figures 5 and 6, the phase behavior and morphology are characterized as follows. (1) The macrophase separation into β-rich lamellar phase (L_2) and α-rich lamellar phase (L_1) occurs rather than that into Dis_2 and L_1. (2) This macrophase separation occurs in the blend composition range of $0.02 \le \Phi_\alpha \le 0.6$, and at $\Phi_\alpha = 0.01$ all of the α copolymer dissolve into β_2 and the macrophase separation does not occur. While in the case of the α/β_1 blend, even 1 wt % of α copolymer causes the macrophase separation. (3) The morphology of the β_2-rich phase is basically lamellar although locally disordered regions are left, while in the α/β_1 blend the β_1-rich phase is in the disordered state. This difference is also observed in the neat β_1 and β_2 copolymers and due to the slight difference in their molecular weights. (4) As for the lamellar spacing of L_1, those of the 5/95 and 20/80 blend are slightly larger than that of the 60/40 blend (see Figure 6).

(c) α/β_3 Blend Series ($r = 6.9$). The representative TEM and SAXS results of α/β_3 blend are presented in Figures 7 and 8, respectively. In this blend α and β_3 undergo the macrophase separation within the blend composition range of $0.02 \le \Phi_\alpha \le 0.5$, suggesting that

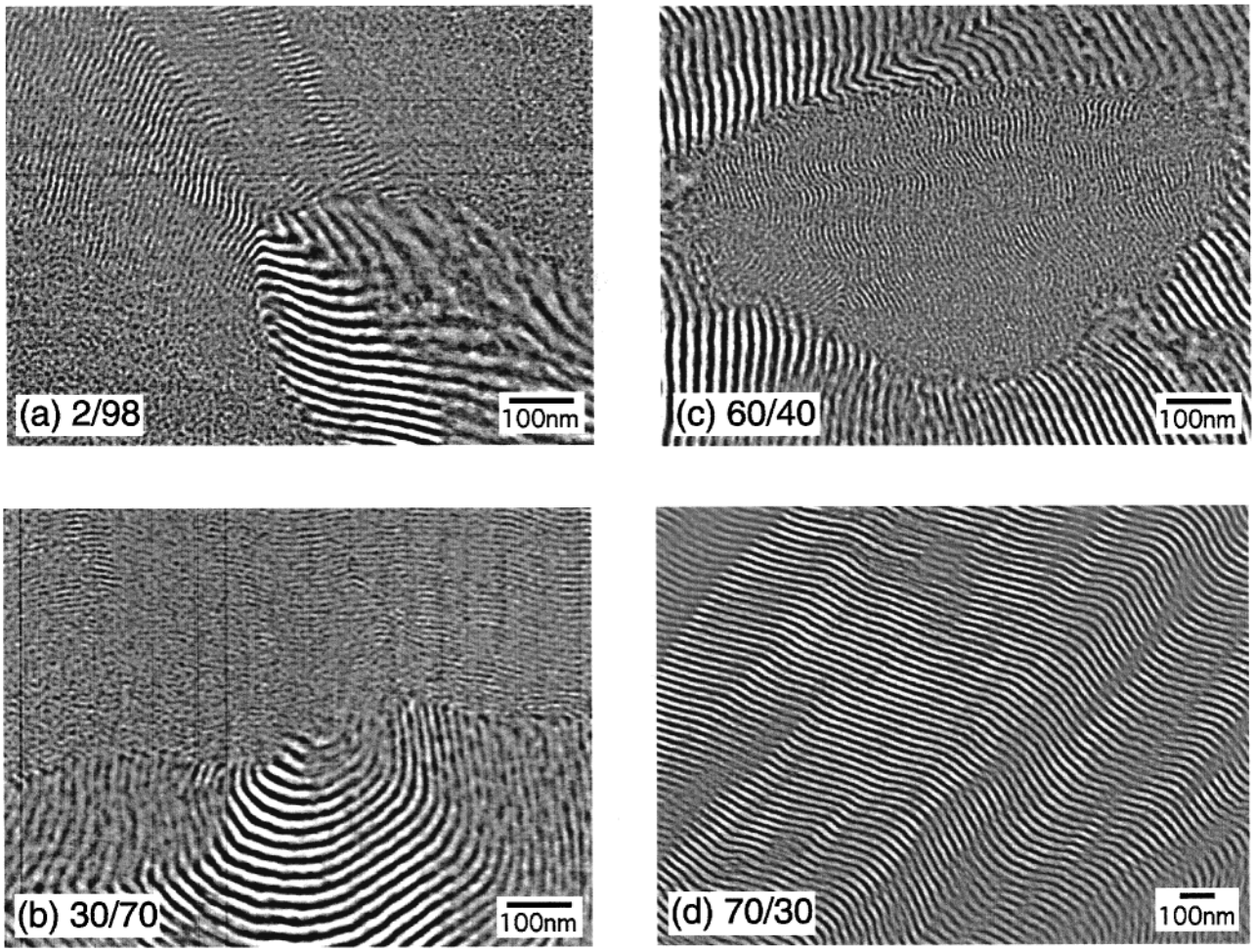

Figure 5. TEM micrographs of α/β_2 blends ($r = 7.4$). The blend compositions are designated in wt %. (a) 2/98 blend; (b) 30/70 blend; (c) 60/40 blend; (d) 70/30 blend.

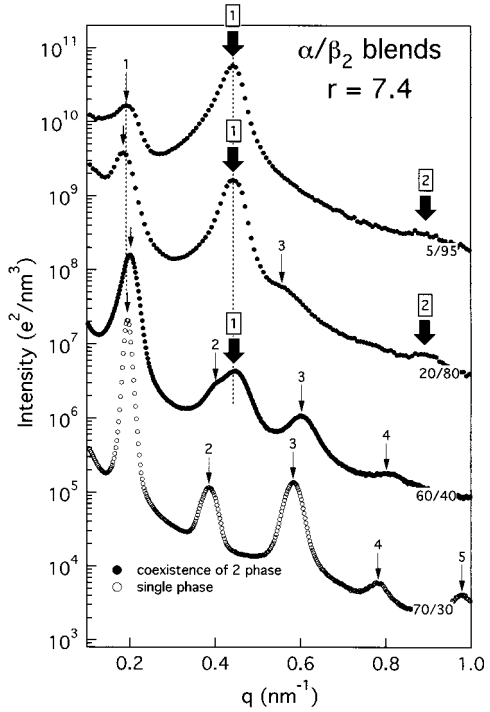

Figure 6. SAXS profiles of α/β_2 blends ($r = 7.4$). The profiles of 5/95, 20/80, and 60/40 blends have been shifted vertically relative to that of 70/30 blend by the factor of 5×10^4, 10^3, and 20, respectively, for clarity. Details are the same as Figure 4 except for the replacing β_1 with β_2.

the totally miscible blend composition range becomes wider as r decreases. Moreover, quite interestingly PS cylindrical (C) morphology appeared within the blend composition range of $0.02 \leq \Phi_\alpha \leq 0.6$. As shown in Figure 7, in the 70/30 blend α and β_3 are totally miscible and form the lamellar (L_1) morphology, while in the 60/40 blend α and β_3 are still totally miscible and form the C morphology. The C morphology in the 60/40 blend is also confirmed by SAXS, as shown in Figure 8. Although a possible interpretation for forming the cylindrical morphology was described in detail elsewhere,[36,37] it will be discussed later in this paper as well. Then further increasing the weight fraction of β_3, α, and β_3 undergo macrophase separation, into the α-rich C phase and β_3-rich phase, whose morphology is alternating lamellae (L_2). This macrophase separation into C and L_2 phases is confirmed by SAXS (see Figure 8) as well. The Bragg spacing of the C phase appears almost independent of the blend composition over the range $0.05 \leq \Phi_\alpha \leq 0.6$. Further discussion will be described in the section IV.3.

(d) α/β_4 Blend Series ($r = 4.8$). In the α/β_4 blends, namely, as r decreases to 4.76, the totally miscible blend composition range is much wider than that of other blends (i.e., $r = 8.3-6.9$), and α and β_4 undergo macrophase separation only in the composition range $0.2 \leq \Phi_\alpha \leq 0.3$ as presented in Figures 9 and 10. Further, similar to the α/β_3 blend, the PS cylindrical morphology (C) is observed in the wide blend composition range of $0.2 \leq \Phi_\alpha \leq 0.6$, which is discussed in the following section. The Bragg spacing of the α-rich phase is

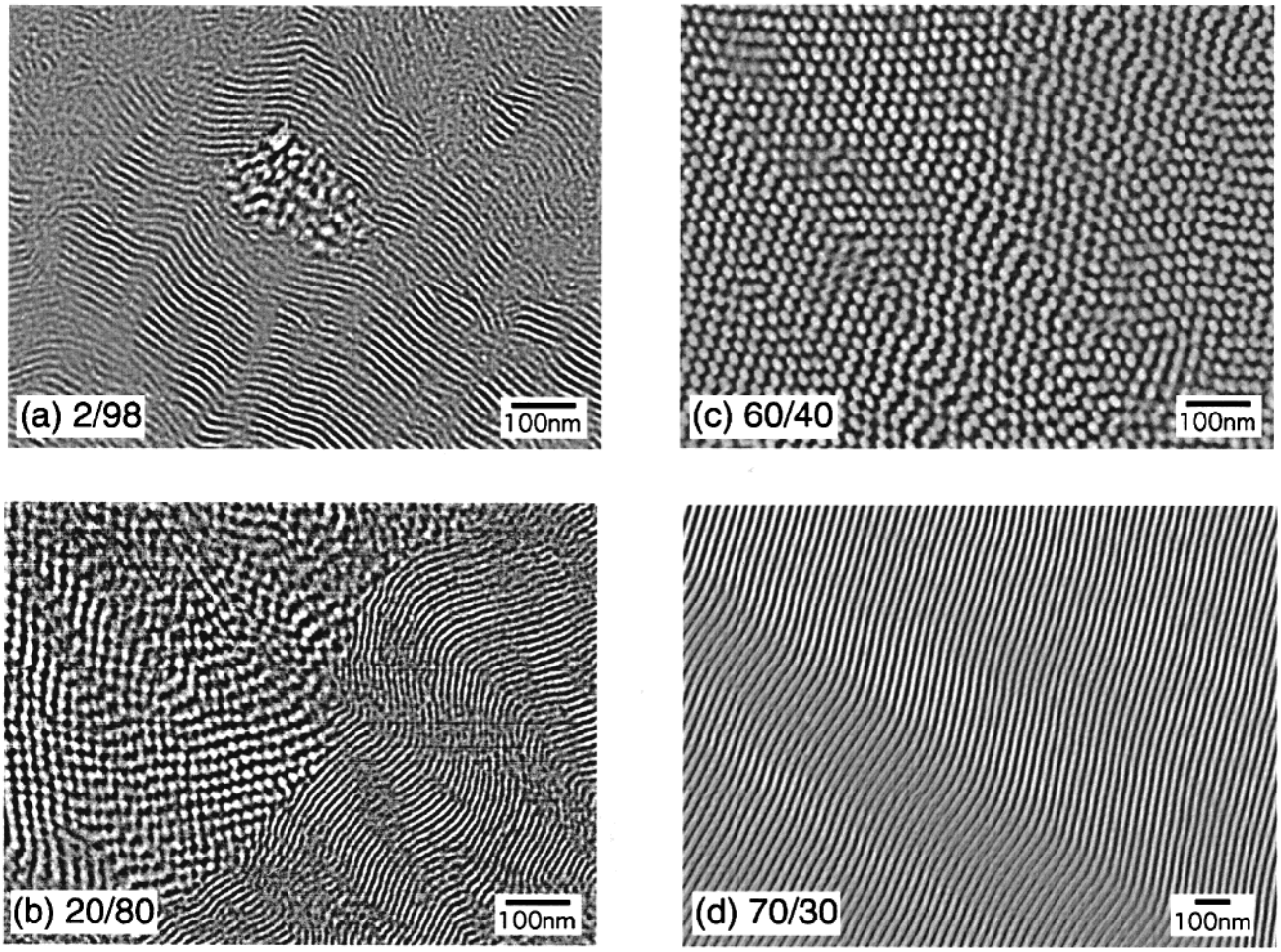

Figure 7. TEM micrographs of α/β_3 blends ($r = 6.9$). The blend compositions are designated in wt %. (a) 2/98 blend; (b) 20/80 blend; (c) 60/40 blend; (d) 70/30 blend.

Table 2. Previous Studies on the Miscibility Criteria for the Binary Blends of A−B Copolymers with Nearly Symmetric Compositions and Different Molecular Weights

specimen code $(A-B)_\alpha/(A-B)_\beta$	copolymer type A−B[a]	total mol wt of α and β $M_{n,\alpha}/M_{n,\beta}$	ratio r[b]	immiscible range[c]	ref
HS-10/HK-7	PS−PI	81400/31900	2.6	*d*	13
HY-10/HY-8	PS−PI	164000/31600	5.2	*d*	13
HS-10/HK-17	PS−PI	81400/8500	9.6	$\Phi_\alpha <$ ca. 0.7[e]	13
HS-9/HS-10	PS−PI	1030000/81400	12.7	$\Phi_\alpha \leq 0.7$[e]	13
HY-12/HY-8	PS−PI	534000/31600	16.9	$\Phi_\alpha <$ ca. 0.7[e]	13
A/M	PS−PI	54000/1800	30	*d*	26
SI120/SI68	PS−PI	120000/68000	1.8	*d*	27
SI120/SI54	PS−PI	120000/54000	2.2	*d*	27
SI120/SI40	PS−PI	120000/40000	3	*d*	27
SI120/SI24	PS−PI	120000/24000	5	*d*	27
SI120/SI12	PS−PI	120000/12000	10	$\Phi_\alpha \leq 0.7$[e]	27
SB07/SB12	PS−PB	148000/22100	6.7	$0.05 \leq \Phi_\alpha \leq 0.6$	28
SB07/SB11	PS−PB	148000/18300	8.1	$0.05 \leq \Phi_\alpha \leq 0.7$	28
SB07/SB05	PS−PB	148000/9200	16.1	$0.02 \leq \Phi_\alpha \leq 0.7$	28

[a] PS, PI, and PB denote polystyrene, polyisoprene, and polybutadiene, respectively. [b] $r = M_{n,\alpha}/M_{n,\beta}$. $M_{n,\alpha}$ and $M_{n,\beta}$ are the number-average molecular weights of α- and β-chain, respectively. [c] Φ_α denotes the volume fraction of α-chain in the blends, which is regarded to be identical with the weight fraction of α-chain since in these studies the copolymer density of α-chain is nearly equal to that of β-chain. [d] At all of the blend compositions α- and β-chain are totally miscible. [e] The lower limit of Φ_α for the immiscible range was not clearly identified.

identical between the 20/80 and the 30/70 blends, while in the 40/60 blend it is larger than that of the 20/80 or the 30/70 blend, as seen from Figure 10.

IV. Discussion

In Figure 11, we summarize the phase diagram of α/β_i ($i = 1-4$) blends in the parameter space of r and Φ_α. Each phase is labeled Dis_2 (disordered state formed by almost pure β-chains), L_2 (lamellar morphology formed in the β-rich phase), L_1 (lamellar morphology formed in the α-rich phase), or C (PS cylindrical morphology formed in the α-rich phase). Since the specimens employed to construct this phase diagram were annealed at 120 °C and then cooled gradually to ambient temperature, we cannot specify the exact temperature for to which this phase diagram (or the phase diagram

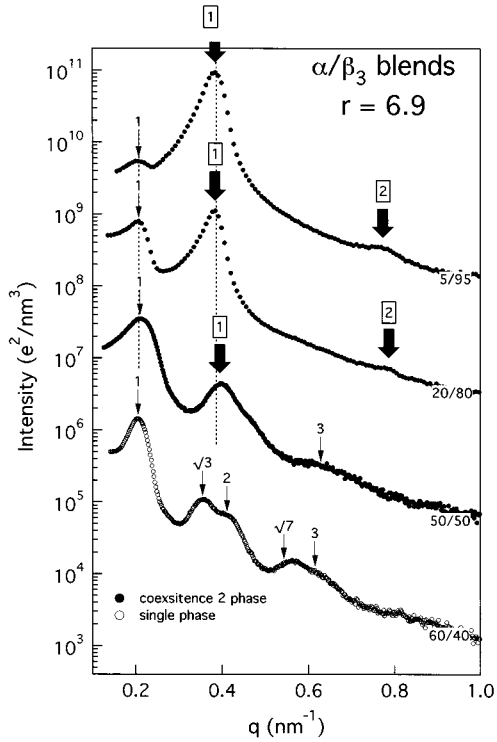

Figure 8. SAXS profiles of α/β_3 blends ($r = 6.9$). The profiles of 5/95, 20/80, and 50/50 blends have been shifted vertically relative to that of 60/40 blend by the factor of 1.25×10^5, 2.5×10^3, and 50, respectively, for clarity. Details are the same as those in Figure 4 except for the replacing β_1 with β_3. The profile of the 60/40 blend clearly shows the existence of hexagonally packed cylinders.

shown in Figure 13) corresponds. However, the following remark is worthy to note: the T_g of the PS microdomains of α-rich phase is around 100 °C; hence, the morphologies of α-rich phases were fixed at around 100 °C. While in the β_i ($i = 1-4$)-rich phase the T_g of PS-rich domains is lowered due to the small molecular weight of PS block and exist at around 60−70 °C. Therefore, the phase diagram of Figures 11 and 13 corresponds to those between 60 and 100 °C. The following two points seem to be worthy of being discussed in this phase diagram: (i) The change of the miscibility criterion between α and β_i copolymers with varying r. (ii) The origin of PS cylindrical morphology observed in α/β_3 and α/β_4 blends. Furthermore, in Figure 16 the Bragg spacing, D, of both α-rich and β_i-rich phases are plotted as a function of Φ_α for all the α/β_i ($i = 1-4$) blends. We will discuss about this issue in section IV.3.

IV.1. Miscibility Criterion. In this section we compare the results of α/β_i ($i = 1-4$) blends with those of literature works.[13,26−28] The representative results of previous experimental studies are summarized in Table 2, concerning the miscibility criteria of two types of A−B copolymers, which have nearly symmetric compositions and different molecular weights. We discern that the results of this study reasonably fit to those of previous studies.[13,26−28]

In generalizing all of the data, the following are features of miscibility criterion of nearly symmetric copolymers: (1) In the regime of $r \leq 5$ the two copolymers are essentially miscible at all the blend compositions. Although the α/β_4 blend in this study, with $r = 4.8$ (slight smaller than 5), has a very narrow miscibility gap (i.e., immiscible blend composition range) of $0.2 \leq \Phi_\alpha \leq 0.3$, such a discrepancy is trivial. (2) In the relatively narrow range of $5 \leq r \leq 7$ the miscibility gap appears and abruptly expands up to $\Phi_\alpha \leq 0.6$. Here the lower limit of Φ_α is almost zero, e.g., in the case of α/β_3 blend in this study, in which $r = 6.9$, only 0.02 of Φ_α causes the macrophase separation of two copolymers. (3) In the regime of $r \geq 7$, the miscibility gap is almost independent of r and holds $0 \approx \Phi_\alpha \leq 0.6$. It seems interesting to note that the miscibility gap is asymmetric with respect to $\Phi_\alpha = 0.5$, namely, in the β-rich phase the α-chains are hardly dissolved, whereas in the α-rich phase the β-chains can be dissolved to some extent. The β-chains, which are dissolved into α-rich phase, localize at the interface of microdomains as "cosurfactants" and reduce the stretching free energy of α-chains[38] (see Figure 12a). (4) In the case that the value of r further increases by decreasing the molecular weight of β-chains, such as the A/M blend in ref 26 (see Table 2), the β-chains become in a deeply disordered state, act as a nonselective solvent, and can be dissolved into the α-chains as shown in Figure 12b. Therefore, the total miscibility between α- and β-chains at any blend compositions is recovered. However, if molecular weight of β further increases keeping $r = 30$, the situation will be same as the case of (3). Thus, the miscibility is generally a function of not only on r but also molecular weight of β for a large value of r. Such a scenario is in good agreement with the theoretical study by Matsen[25] (compare Figure 1 or Figure 2 of ref 25 with Figure 13). Figure 13 schematically summarizes the above scenario except for the results of $r = 30$ with the exceptionally short β. The figure includes also the single phase with the nonlamellar morphology formed in this work.

IV.2. PS Cylindrical Morphology Formed by Mixing Lamellar-Forming Block Copolymers. One of the most interesting and characteristic features in the phase diagram of this study is the formation of PS cylindrical morphology at a certain blend compositions of α/β_3 ($r = 6.9$) and α/β_4 ($r = 4.8$) blends (Figures 11 and 13). It should be noted that one example of nonlamellar morphology was previously reported in HS-10/HK-7 blends of ref 13, and that there are some common tendencies between the present study and the previous study, as will be described in the following: (1) The constituent copolymers, especially β-chains, have an asymmetry in their composition to some extent, although they are, by themselves, self-assembled into lamellar morphology. (2) The nonlamellar morphologies tend to appear when the small amount of α-chain is added to the neat β-chains, and these morphologies are maintained up to $\Phi_\alpha \cong 0.5$ (for HS-10/HK-7) or $\Phi_\alpha \cong 0.6$ in this study. On the other hand, when the α-chain is the major component, i.e., in the blend composition range of $\Phi_\alpha \geq 0.7$, the lamellar morphology is retained.

From these trends mentioned above we can make the following scenario as for the formation of the cylindrical morphology. In this case the β-chain has a slight asymmetric composition so that its spontaneous curvature is not zero (Figure 14a). However, the neat β-chains cannot be self-assembled into the cylindrical morphology, because the radii of cylinders, if cylinders were formed, are too small compared with those expected from the spontaneous curvature inherent in the β-chain or the mean curvature of the cylindrical domain (shown by solid line) is too large compared with the spontaneous curvature shown in broken lines (Figure 14b). Conse-

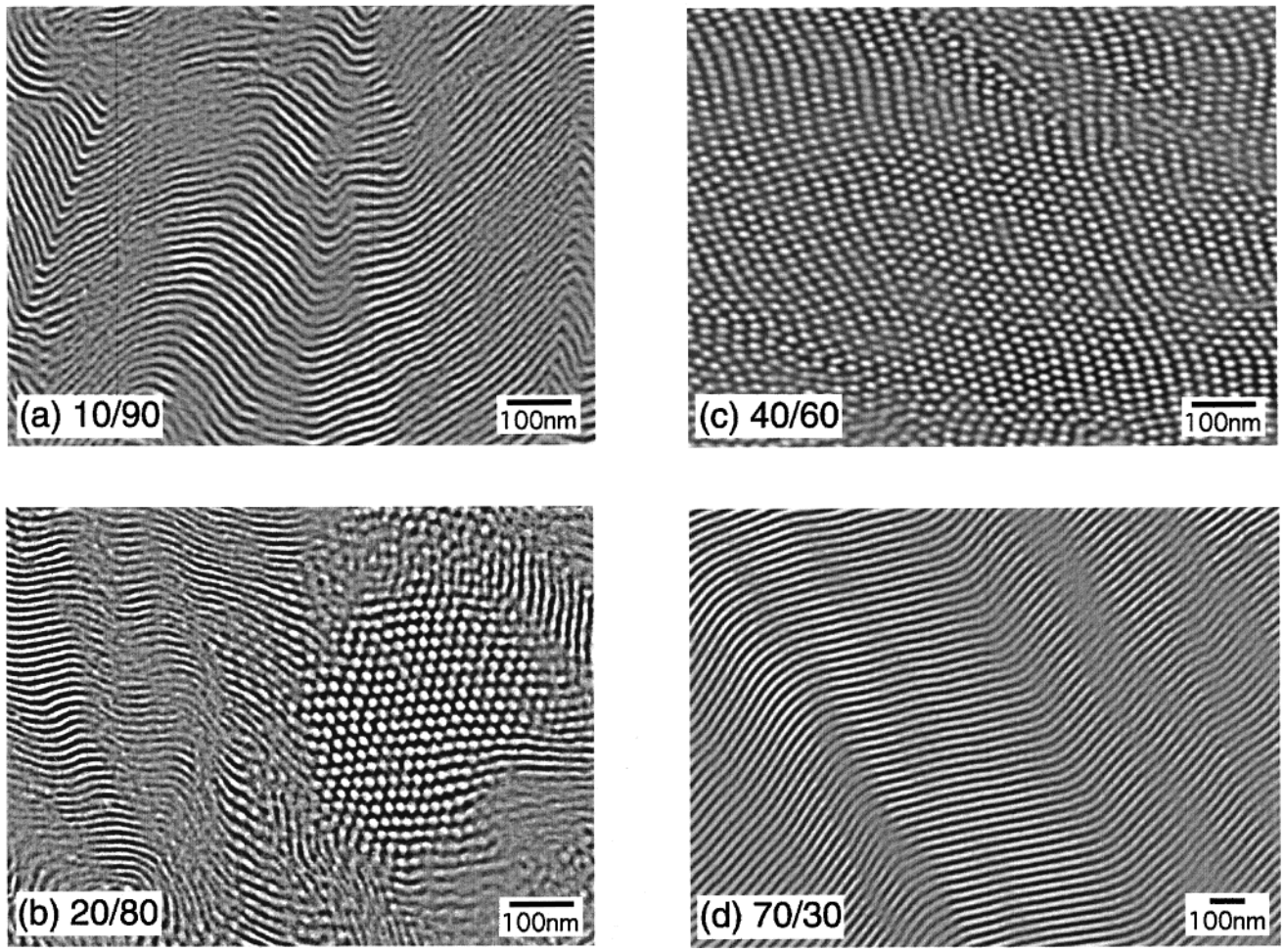

Figure 9. TEM micrographs of α/β_4 blends ($r = 4.8$). The blend compositions are designated in wt %. (a) 10/90 blend; (b) 20/80 blend; (c) 40/60 blend; (d) 70/30 blend.

quently, the neat β-chains are self-assembled into lamellar morphology, and the spontaneous curvature inherent in the β-chain vanishes. Then, let us suppose that a small number of α-chains are added to β-chains, and they can be miscible with β-chains and cooperate in forming a microdomain. In such a situation the cylinders with large radii can be formed because the segments of α-chain can fill the central part of the cylinder domain, and the cylinders whose mean curvature is close to the spontaneous curvature inherent in the β-chain will be realized (Figure 14c). In general, the less the asymmetry in the composition of β-chain, the larger molecular weight of α-chain is required to allow formation of cylinders. However, in such a case, r is too large and macrophase separation between α- and β-chains occurs before the formation of cylinders. Therefore, it seems reasonable to consider that the formation of cylinders most easily happen in the range of $5 \leq r \leq 7$, in which the miscibility between α- and β-chains abruptly change.

Furthermore, we have examined this phenomenon more quantitatively by using the theory developed by Lyatskaya et al. (BZL model).[37,38] Here only the calculation result of free energy for the α/β_4 blend is shown in Figure 15, and the parameters used for the calculation are summarized in Tables 3 and 4. The details of the calculation and the calculation result for α/β_3 blend have been already shown elsewhere.[36] It should be noted that in the calculation we have incorporated the asymmetry in segmental volume as well as conformation (i.e., Kuhn length) between PS and PI.[36] In Figure 15 the vertical axis is the reduced value of $\Delta F_x/\Phi$ to preclude evaluation of Φ where ΔF_x denotes the free energy per chain in the case of morphology x (x = lamellar or PS cylindrical) and Φ denotes the free energy of interfacial area per

Table 3. Characteristics of Polymerization Indices of the PS and PI Blocks for the Two Block Copolymers FS-1 and H102 Used for Calculations

i	N^i_{PS} [a]	N^i_{PI} [a]	$\bar{N}^i_{PS}$ [b]	$\bar{N}^i_{PI}$ [b]
FS-1	87	176	99.5	153.8
H102	481	735	550.3	642.4

[a] N^i_{PS} and N^i_{PI} are number-average degree of polymerizations of polystyrene and polyisoprene block chains and given as $N^i_{PS} = M_n(PS)/104$ and $N^i_{PI} = M_n(PI)/68$, respectively. [b] $\bar{N}^i_j$ (j = PS or PI) is given by eq 29 of ref 36.

Table 4. Relative Difference in the PS and PI Block Length α_j between the Two Block Copolymers FS-1 and H102 and the Stiffness Parameter of PS and PI Block Chains p_j

j	α_j[a]	p_j[b]
PS	4.53	1.16
PI	3.18	1.26

[a] α_j (j = PS or PI) is given by eq 7 of ref 36. [b] p_j (j = PS or PI) is given by $p_j = A_j/a$, where A_j is the Kuhn statistical segment length of jth polymer based on a common segment volume of a^3. Here we used $A_{PS} = 5.5$ Å and $A_{PI} = 6.0$ Å, based on a common segment volume of $a^3 = 1.08 \times 10^{-22}$ cm^3 in accordance with ref 36.

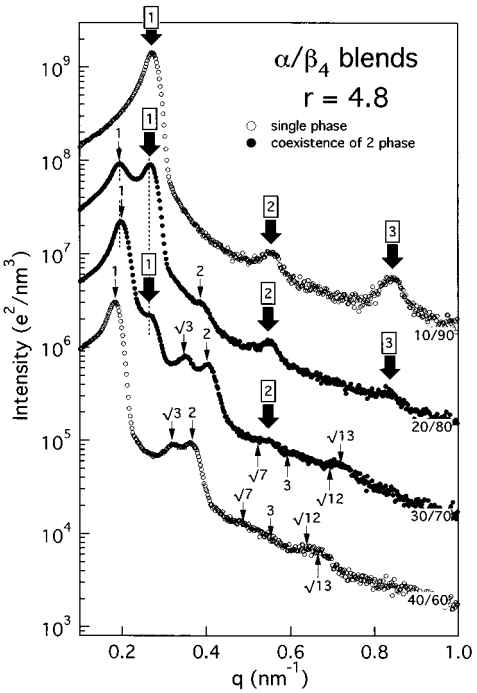

Figure 10. SAXS profiles of α/β_4 blends ($r = 4.8$). The profiles of 10/90, 20/80, and 30/70 blends have been shifted vertically relative to that of 40/60 blend by the factor of 1×10^3, 1×10^2, and 10, respectively, for clarity. Details are the same as those in Figure 4 except for the replacing β_1 with β_4. The profile of the 40/60 blend clearly shows existence of hexagonally packed cylinders.

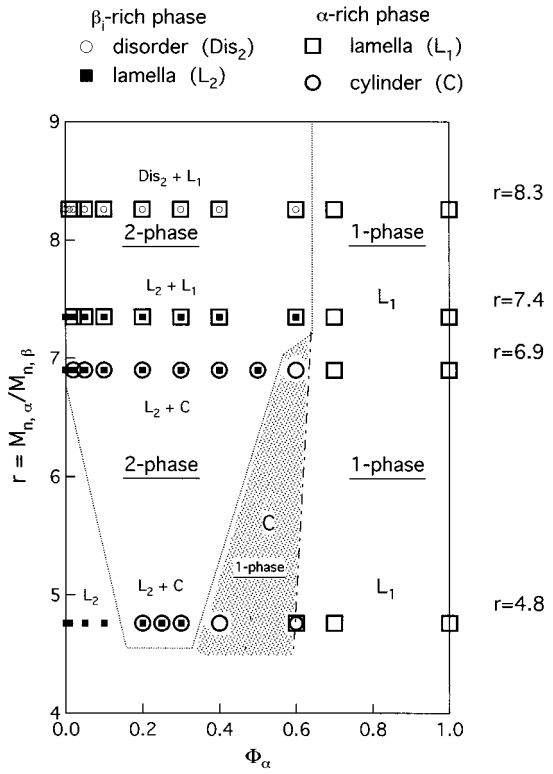

Figure 11. Phase diagram of α/β_i blends ($i = 1-4$) in the parameter space of the molecular weight ratio (r) and the weight fraction of α-copolymer (Φ_α). The single phase of PS-cylindrical morphology was observed in the shaded area.

unit segment area between PS and PI domains, which is considered to be independent of the morphology. The following observations are worthy to be noted. Although the free energy curves of lamella and PS cylinder do not intersect, implying that lamella is the stable morphology at any blend compositions, the free energy difference of the blend at $\Phi_\alpha = 0.4$ is much smaller than those at $\Phi_\alpha = 0.1$ or 0.7. Therefore, the calculation successfully predicted that blending of α and β_4 can lower the free energy of the cylindrical morphology very effectively at the experimentally relevant blend composition. The lack of success in predicting the stable cylindrical morphology might be due to the inaccuracies in the theory and some degree of experimental errors in the parameters used for the calculation.

Another point of interest about this calculation is to actually answer how strongly the choice of the parameters influences the values of the free energy. To answer this question, we calculated the free energy curves of lamellar and PS cylindrical morphology with varying PS volume fraction of short diblock copolymer (i.e., $f_{PS,\beta}$) in the cases of $f_{PS,\alpha} = 0.47$ and $r = 6.9$ or 4.8, which correspond to α/β_3 or α/β_4 blends, respectively, and searched for the range of $f_{PS,\beta}$ where the morphology transition between lamella and PS cylinder occurs. As a result, we found that in the case of $r = 6.9$ the morphological transition occurs in the range of $f_{PS,\beta} \leq 0.39$, while in the case of $r = 4.8$ the transition occurs

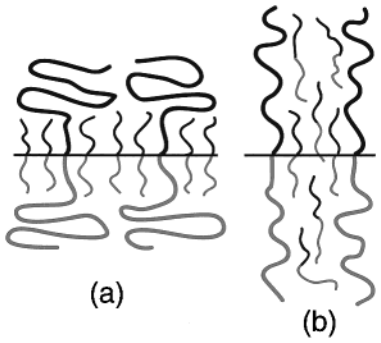

Figure 12. Schematic representation for the short block copolymer chain dissolved in the ordered long block copolymer-rich phase. (a) All of the short copolymer chains are localized at the microdomain interface. (b) Some of short copolymer chains are delocalized from the microdomain interface and swell the microdomains.

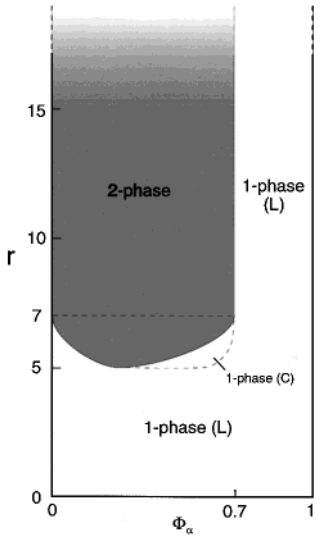

Figure 13. Schematic phase diagram for the binary blends of A−B diblock copolymers with nearly symmetric compositions but different molecular weights. This phase diagram captures the common features of previous studies (refs 13, 27, and 28) and this study except for the blend having $r = 30$ in Table 2.

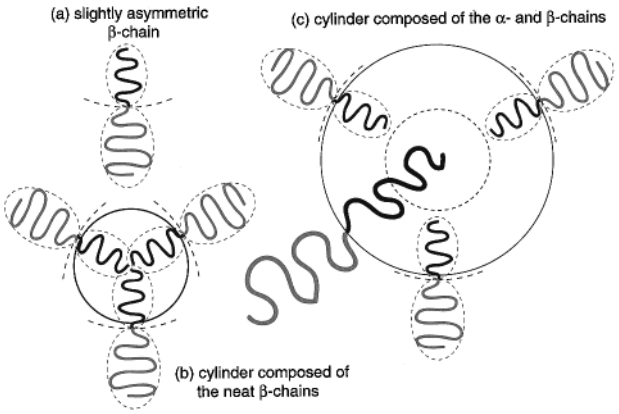

Figure 14. Schematic illustration for the formation of the cylindrical morphology. (a) A molecule of slightly asymmetric diblock copolymer (β-chain) with nonzero spontaneous curvature. (b) Cylindrical morphology formed by neat β-chains shown in part (a). In this case the mean curvature of the cylinder (solid line) is larger than the spontaneous curvature of β-chain (dashed lines). (c) Cylindrical morphology formed by the binary blend of β-chains shown in part a and large symmetric copolymers (α-chain). In this case the mean curvature of cylinder closely fits to the spontaneous curvature of β-chain.

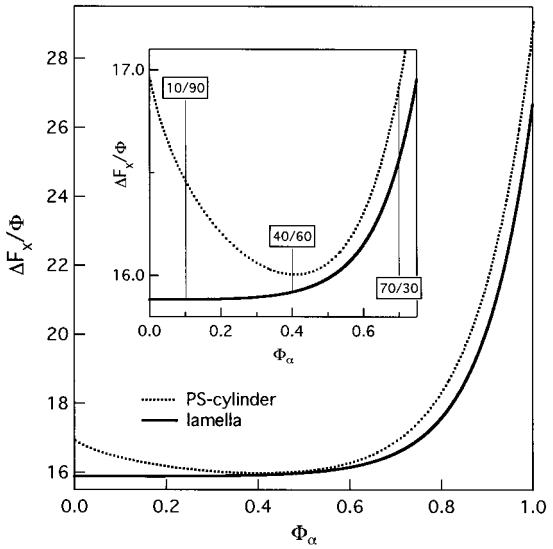

Figure 15. Results of model calculations for free energies of lamellar (solid line) and PS cylindrical morphology (dashed line). The reduced free energy ($\Delta F_x/\Phi$) as a function of Φ_α.

in the range of $f_{PS,\beta} \leq 0.38$. Furthermore, when we examined the case of $f_{PS,\alpha} = 0.47$ and $r = 10$, the range where the transition occurs extended to $f_{PS,\beta} \leq 0.41$. Therefore, we could show the tendency that the cylindrical morphology appears more easily with increasing r.

IV.3. Variation of *D* for Both α- and *β*-Rich Phases with Φ_α. In Figure16, which summarizes the D spacings for α/β_i ($i = 1-4$) with Φ_α, the following observations are worthy of note. At $\Phi_\alpha = 0.7$, D decreases with the average molecular weight of the blend specimen, namely (D for α/β_4) > (D for α/β_3) > (D for α/β_2) > (D for α/β_1). This tendency seems rational, suggesting that at $\Phi_\alpha = 0.7$ all the blends α and β_i ($i = 1-4$) are totally miscible and form the uniform microdomains whose sizes depend on the average molecular weights of the blends.

With further decreasing of Φ_α from 0.7, all the blends undergo macrophase separation, in the concentration

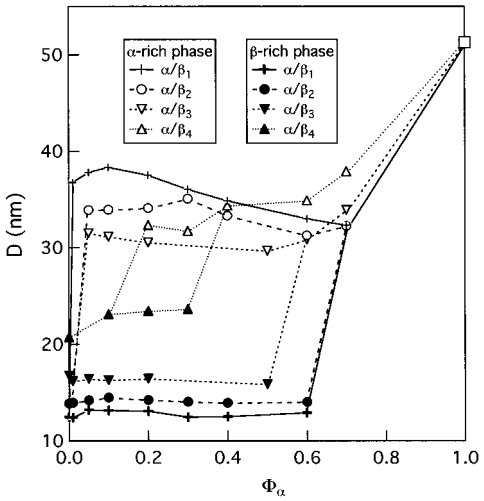

Figure 16. Bragg spacing, D, plotted as a function of Φ_α. D of the α-rich phase is denoted by open symbol, while D of the β-rich phase is denoted by filled symbol. (+) α/β_1 blend; (○, ●) α/β_2 blend; (▽, ▼) α/β_3 blend; (△, ▲) α/β_4 blend.

range $\Phi_{1,c} \leq \Phi_\alpha \leq \Phi_{2,c}$ where $\Phi_{1,c}$ and $\Phi_{2,c}$ are the system-dependent critical concentration of Φ_α for the macrophase separation, and hence have two values of D, D_α and D_β for the domains rich in α and β, respectively. The value D_β is nearly independent of Φ_α and close to that for the neat β, except for α/β_4, simply because β domains hardly dissolve the α chains. However, the behavior of D_α is different for each blend. In the case of the α/β_1 with $r = 8.3$ and α/β_2 with $r = 7.4$, D_α increases with decreasing Φ_α. This tendency is counterintuitive since the average molecular weight decreases with decreasing Φ_α. In fact, the totally miscible blends of the block copolymers in the previous studies[13,27] showed the monotonic decrease of the lamellar spacing with decreasing of Φ_α. The tendency that D increases with decreasing Φ_α is less outstanding for α/β_2. In the case of α/β_3 with $r = 6.9$, D_α is almost independent of Φ_α, while D_α tends to decrease with decreasing Φ_α for α/β_4 with 4.8.

The variation of D_α with Φ_α in the two-phase region ($\Phi_{1,c} \leq \Phi_\alpha \leq \Phi_{2,c}$) is puzzling, from a viewpoint that the equilibrium volume fraction of β dissolved in the α-rich phase should be independent of Φ_α and hence D_α should be independent of Φ_α. This point should be clarified in future. The critical volume fraction of Φ_α ($\Phi_{1,c}$ and $\Phi_{2,c}$) for the miscibility gap shows an interesting molecular weight and/or molecular weight ratio dependence, which is worthy to be compared with theoretical predictions in the future.

V. Concluding Comments

In this study we examined the phase behavior of the binary mixtures of PS−PI copolymers having nearly symmetric copolymer composition but different total molecular weight, intensively in the range of $5 \leq r \leq 10$. Here r denotes the molecular weight ratio of the larger copolymer chain to the smaller copolymer chain. Two features were observed: (i) The large and small copolymers become immiscible in the vicinity of $r = 5$, and the miscibility gap (i.e., the immiscible blend composition range) expands to $0 \approx \Phi_\alpha < 0.7$ with the increase of r from 5 to 7 where Φ_α denotes the volume fraction of large copolymer. (ii) In the range of $5 \leq r \leq 7$, nonlamellar morphology is easily appeared in the

blend specimens due to the slight asymmetry in the composition of the small copolymer.

Acknowledgment. We thank Dr. Mikihito Takenaka, Professor Toshihiro Kawakatsu, and Dr. Hiroshi Morita for very useful suggestions and discussions. This work was financially supported in part by a Grant-in-Aid for Scientific Research (under Grant 12305060(A) and Grant 12640392(C)) from the Ministry of Education, Science and Culture, Japan, and by the national project, which has been entrusted to the Japan Chemical Innovation Institute (JCII) by the New Energy and Industrial Technology Development Organization (NEDO) under MITI's Program for the Scientific Technology Development for Industries that Creates New Industries.

References and Notes

(1) Hamley, I. W. *The Physics of Block Copolymers*; Oxford University Press: Oxford, 1998, and references therein.
(2) Hashimoto, T. In *Thermoplastic Elastomers, A Comprehensive Review*; Legge, N. R., Holden, G., Schroeder, H. E., Eds.; Hanser: Munich, 1996; p 429.
(3) Hasegawa, H.; Hashimoto, T. In *Comprehensive Polymer Science, Second Supplement*; Aggarwal, S. L., Russo, S., Vol. Eds.; Pergamon: New York, 1996; p 497.
(4) Bates, F. S.; Fredrickson, G. H. *Annu. Rev. Phys. Chem.* **1990**, *41*, 525.
(5) Hashimoto, T.; Tanaka, H.; Hasegawa, H. *Molecular Conformation and Dynamics of Macromolecules in Condensed Systems*; Nagasawa, M., Ed.; Elsevier: Amsterdam, 1988; p 257.
(6) Bates, F. S.; Fredrickson, G. H. *Phys. Today* **1999**, *52*, 32.
(7) Birshtein, T. M.; Zhulina, E. B.; Polotsky, A. A.; Abetz, V.; Stadler, R. *Macromol. Theor. Simul.* **1999**, *8*, 151.
(8) Goldacker, T.; Abetz, V.; Stadler, R.; Erukhimovich, I. Ya.; Leibler, L. *Nature* **1999**, *398*, 137.
(9) Goldacker, T.; Abetz, V. *Macromolecules* **1999**, *32*, 5165.
(10) Goldacker, T.; Abetz, V. *Macromol. Rapid Commun.* **1999**, *20*, 415.
(11) Abetz, V.; Goldacker, T. *Macromol. Rapid Commun.* **2000**, *21*, 16.
(12) Goldacker, T.; Abetz, V.; Stadler, R. *Macromol. Symp.* **2000**, *149*, 93.
(13) Hashimoto, T.; Yamasaki, K.; Koizumi, S.; Hasegawa, H. *Macromolecules* **1993**, *26*, 2895.
(14) Hashimoto, T.; Koizumi, S.; Hasegawa, H. *Macromolecules* **1994**, *27*, 1562.
(15) Koizumi, S.; Hasegawa, H.; Hashimoto, T. *Macromolecules* **1994**, *27*, 4371.
(16) Nakai, A.; Wang, W.; Hashimoto, T.; Blumstein, A.; Maeda, Y. *Macromolecules* **1994**, *27*, 6963. Nakai, A.; Wang, W.; Hashimoto, T.; Blumstein, A. *Macromolecules* **1996**, *29*, 5288.
(17) Mayes, A. M.; Russell, T. P.; Deline, V. R.; Satija, S. K.; Majkrzak, C. F. *Macromolecules* **1994**, *27*, 7447.
(18) Koneripalli, N.; Levicky, R.; Bates, F. S.; Matsen, M. W.; Satija, S. K.; Ankner, J.; Kaiser, H. *Macromolecules* **1998**, *31*, 3498.
(19) Yamaguchi, D.; Bodycomb, J.; Koizumi, S.; Hashimoto, T. *Macromolecules* **1999**, *32*, 5844.
(20) Shi, A.-C.; Noolandi, J. *Macromolecules* **1994**, *27*, 2936.
(21) Spontak, R. J. *Macromolecules* **1994**, *27*, 6363.
(22) Shi, A.-C.; Noolandi, J.; Hoffmann, H. *Macromolecules* **1994**, *27*, 6661.
(23) Court, F. These de Doctorat de l'Université Pierre et Marie Curie, 1996.
(24) Court, F.; Hashimoto, T. *Macromolecules* **2001**, *34*, 2536.
(25) Matsen, M. W. *J. Chem. Phys.* **1995**, *103*, 3268.
(26) Lin, E. K.; Gast, A. P.; Shi, A.-C.; Noolandi, J.; Smith, S. D. *Macromolecules* **1996**, *29*, 5920.
(27) Kane, L.; Satkowski, M. M.; Smith, S. D.; Spontak, R. J. *Macromolecules* **1996**, *29*, 8862.
(28) Papadakis, C. M.; Mortensen, K.; Posselt, D. *Eur. Phys. J. B* **1998**, *4*, 325.
(29) Koga, T.; Koga, T.; Hashimoto, T. *J. Chem. Phys.* **1999**, *110*, 11076.
(30) Fujimura, M.; Hashimoto, T.; Kawai, H. *Mem. Fac. Eng., Kyoto Univ.* **1981**, *43* (2), 224.
(31) Hashimoto, T.; Suehiro, S.; Shibayama, M.; Saijo, K.; Kawai, H. *Polym. J.* **1981**, *13*, 501.
(32) Suehiro, S.; Saijo, K.; Ohta, Y.; Hashimoto, T. *Anal. Chim. Acta* **1986**, *189*, 41.
(33) Hendricks, R. W. *J. Appl. Crystallogr.* **1972**, *5*, 315.
(34) Kato, K. *J. Polym. Sci., Polym. Lett. Ed.* **1996**, *4*, 35.
(35) Ribbe, A. E.; Bodycomb, J.; Hashimoto, T. *Macromolecules* **1999**, *32*, 3154.
(36) Yamaguchi, D.; Shiratake, S.; Hashimoto, T. *Macromolecules* **2000**, *33*, 8258.
(37) Lyatskaya, J. V.; Zhulina, E. B.; Birshtein, T. M. *Polymer* **1992**, *33*, 343.
(38) Birshtein, T. M.; Liatskaya, Y. V.; Zhulina, E. B. *Polymer* **1990**, *31*, 2185. Zhulina, E. B.; Birshtein, T. M. *Polymer* **1991**, *32*, 1299.

MA0021489